Journal of Ovonic Research Vol. 16, No. 2, March - April 2020, p. 115 - 122

MODELING OF THE INDIUM GALLIUM NITRIDE TANDEM SOLAR CELL PHOTOVOLTAIC PERFORMANCES FOR CONCENTRATOR

N. BELLAL[a,*], B. DENNAI[b]
[a]*Laboratory of Semiconductor Devices Physics, University Tahri Mohammed of Bechar, Algeria*
[b] *Laboratory of Renewable Energy Development and their Applications in the Saharan areas, Faculty of Exact Sciences, University Tahri Mohammed Bechar*

The objective of this modeling investigation is to optimize a solar cell tandem device under the AM1.5G spectrum, based InGaN cells for concentration ratio.
In this paper describes the role of the concentration photovoltaic in InGaN dual-junction solar cell. this study, the top cell is made of InGaN (1.64 eV) while the bottom cell is made of InGaN (0.94 eV).the reported for purpose was to extracted the solar cell parameters(photocurrent, open circuit voltage and efficiency) in a fairly wide range of concentration levels (1 to30 sun).Our calculation shows that the efficiency can be improved from (23.87%) for a tandem solar cell with (X=1sun) up to (25.72%) for same device solar cell with (X=30sun) for AM.1.5 illumination and room temperature.

(Received November 25, 2019; Accepted March 26, 2020)

Keywords: Solar cell, Concentration ratio, InGaN, tandem, Efficiency

1. Introduction

Photovoltaic solar energy is a renewable energy source capable of producing electricity in large quantities over the long term without emitting greenhouse gases. Several technological advances have been made in recent years to reduce the price of the peak watt of the module and increase its efficiency [1]. Different materials as well as several architectures of solar cells appeared to manufacture a photovoltaic module with high efficiency (tandem architecture) [2]. Indeed, the main parameter limiting the efficiency of solar cells lies in their inadequate absorption spectrum with the incident solar spectrum.

InGaN materials have an interesting moldable gap energy ranging from 0.7 eV to 3.42 eV and a high optical absorption coefficient of more than 105 / cm which indicates better absorption of the solar spectrum [3, 4].These Indium Gallium Nitride (InGaN) solar cells have recently been recognized as serious photovoltaic candidates with the potential for high conversion efficiencies. To achieve the expected objectives of a photovoltaic technology as a competitive energy source compared to fossil fuels, the higher efficiency of conversion of the cell, low cost and stability, are the dominant factors. To adapt the solar radiation to the spectral sensitivity of the PV cells in order to increase their spectral absorption range. The solution is the increase of the power incident on the solar cell by a concentrator.

In this work, we have studied the main properties of anInGaN-based multi-junction solar cell under different concentration ratios (1 sun to 30 suns), using Matlab software. Was illuminated by the AM 1.5d reference spectrum

*Corresponding authors: deennai_benmoussa@yahoo.com

2. Modelling and simulations

2.1. PV characteristic from tandem cell

The total of the photo current density from single cells under illumination is given by [5]:

$$J(\lambda) = J_p + J_n + J_{dr}(\lambda) \tag{1}$$

where: J_n the photo current density in the base region is expressed by:

$$J_n = +qD_n(dn/dx) \tag{2}$$

In the general case, the current comes from both mechanisms. The effects of the electric field and the concentration gradient are superimposed.

We write that:

$$J_n = q\mu_n n\,\varepsilon + qD_n(dn/dx) \tag{3}$$

$$J_n = qD_n\left(\frac{dn_p}{dx}\right)_{x_j+W} = \frac{q\eta(1-R)\alpha L_n}{(\alpha^2 L_n^2 - 1)} exp\left[-\alpha(x_j + w)\right] * \left[\alpha L_n - \frac{\left(\frac{S_n L_n}{D_n}\right)(\cosh\left(\frac{H'}{L_n}\right) - [\exp(-\alpha H')]) + \sinh\left(\frac{H'}{L_n}\right) + \alpha L_n \exp(-\alpha H')}{\frac{S_n L_n}{D_n}\sinh\left(\frac{H'}{L_n}\right) + \cosh\left(\frac{H'}{L_n}\right)}\right] \tag{4}$$

With $H' = H - (x_j + w)$.

J_p The photo current density in the emitter region is expressed by

$$J_p = -qD_p(dp/dx) \tag{5}$$

The current comes from both mechanisms. The effects of the electric field and the concentration gradient:

$$J_p = q\mu_p p\,\varepsilon - qD_p(dp/dx) \tag{6}$$

$$J_p = -qD_p\left(\frac{dp_n}{dx}\right)_{x_j} = \left[\frac{q\eta(1-R)\alpha L_p}{(\alpha^2 L_p^2 - 1)}\right] * \left[\frac{\left(\frac{S_p L_p}{D_p} + \alpha L_p\right) - exp(-\alpha x_j)\left(\frac{S_p L_p}{D_p} cosh\frac{x_j}{L_P} + sinh\frac{x_j}{L_P}\right)}{\frac{S_p L_p}{D_p} sinh\frac{x_j}{L_P} + cosh\frac{x_j}{L_P}} - \alpha L_p exp(-\alpha x_j)\right] \tag{7}$$

The photo current density in space charge layer pn is expressed by

$$J_{dr} = q\eta(1-R)exp\left(-\alpha x_j\right)[1 - exp(-\alpha w)] \tag{8}$$

The open circuit voltage is given by

$$V_{co} = (kT/q)\, ln[(I_{cc}/I_s) + 1] \tag{9}$$

The power supplied to the external circuit by the solar cell under illumination depends on the load resistor (external resistor placed across the cell). This power is maximum for an operating point Pm (Im,Vm) of the current-voltage curve. To this point we can write after approximations

$$V_{mp} = V_{co} - (kT/q)\, log\left[\left(q\, V_{mp}/KT\right) + 1\right] \tag{10}$$

$$I_{mp} = I_{ph} + J_0\, e\left[\left(q\, V_{mp}/KT\right) - 1\right] \tag{11}$$

The cell conversion efficiency is usually taken to be:

$$\eta = V_M I_M / P_i S \tag{12}$$

P_i : is the total incident solar power, S: cell surface. The form factor FF, it determines the electrical quality of the cell.

$$FF = V_M I_M / V_{co} I_{cc} \tag{13}$$

For tandem solar cells and when the cells are connected together by a transparent glue. This adhesive can be either conductive. Should be noted that the same current flows through all the cells and the total voltage across the device is simply the sum of the voltages across each cell. After determining the operating pointI_{mk} , V_{mk} independent cells, we impose a power series I equal to the smallest of the currents I_{mk} whether$I = inf(I_{mk})$. We obtain an operating voltage V_{mk} and useful power:

$$P_k = V_{mk}.inf(I_{mk}) \tag{14}$$

The overall performance will[6]:

$$\eta = \frac{\sum_{k=1}^{n} P_k}{P_{in}} \tag{15}$$

2.3.PV characteristic from tandem solar cells for concentration

An increase in illumination implies an increase in the theoretical efficiency of the cells, if we neglect the losses due to the series resistance Rs and the rise in temperature. the short-circuit current Icc of the cells increases linearly with the concentration, however Vco and FF increase slightly under the effect of the concentration, which produces a net increase in efficiency of the solar cell, assuming that the saturation current at the darkness of the solar cell I_0 is constant under concentration and the parasitic resistances are negligible [7].

$$I_0 = \frac{I_{cc1}}{e^{(qV_{co}/KT)}} \tag{16}$$

With Iccand Vco under a sun is to say without concentration but under a concentration of X times Iccincreases until X *Icctherefore[8], the open circuit voltage under the concentration VcoX becomes:

$$V_{coX} = \frac{KT}{q} \ln\left(\frac{XJ_{cc}}{J_0}\right) \tag{17}$$

The substitution of the equation in and rearrangement gives:

$$V_{coX} = V_{co} + \frac{KT}{q} \ln(X) \tag{18}$$

$$\Delta V_{co} = V_{coX} - V_{co} = \frac{KT}{q} \ln(X) \tag{19}$$

where X is the concentration ratio and ΔVco is the Vcovariation due to the concentration

The increase in Vco also produces a small rise in the FF. The conversion efficiency of the cell under the concentration and the influence of the series resistance are given by the following expression [9].

$$\eta(X) = \frac{J_{cc}(X) V_{co}(X) FF(X)}{X.X_{unsoleil}} \tag{20}$$

with:

$$FF(X) = (FF_{unsoleil} + 0.0035\, ln(X)).\left(1 - \frac{X.J_{ph}R_s}{V_{co}(X)}\right) \quad (21)$$

X: is the concentration rate.
η: The conversion efficiency without concentration.
Icc_1: the current of short circuit under a sun.
Vco_1: The open circuit voltage under a sun.

In practice the electrical efficiency as a function of the concentration begins to increase in accordance with the relation passes through a maximum and decreases. Two causes are at the origin of this limitation, the effect of the temperature and that of the internal resistance of the solar cell [9].

$$X_{maxl}(\eta_{max}) = \frac{V_T}{R_s.J_{ph,unsoleil}} = \frac{0.66\Omega c2}{R_s} \quad (22)$$

3. Device modeling

Fig. 1 shows the schematic diagram of the multi-junction solar cell used in the simulation. The device consists of four regions which are p-$In_{0.52}Ga_{0.48}N$ (emitter), n-$In_{0.52}Ga_{0.48}N$ (base) for top cell and p-$In_{0.84}Ga_{0.16}N$ (emitter), n-$In_{0.84}Ga_{0.16}N$) (base) for bottom cell.

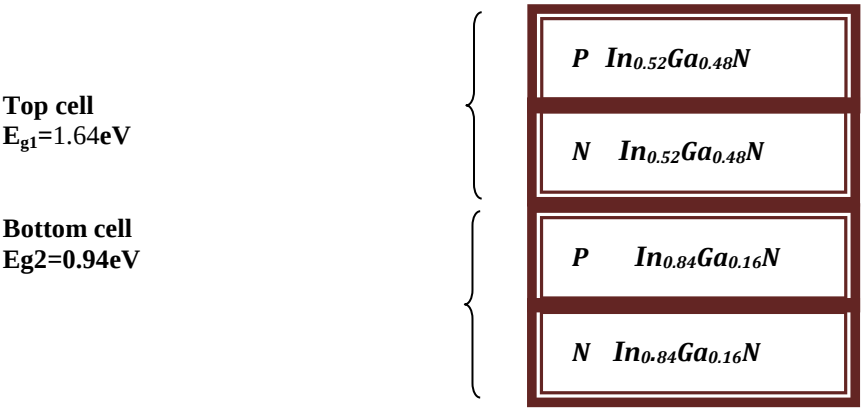

Fig. 1. Cascade tandem solar cell - $In_{0.52}Ga_{0.48}N$/ $In_{0.84}Ga_{0.16}N$structure used for the modeling.

3.2. Parameters for the simulation of $In_xGa_{1-x}N$ soler cell

Material parameter equations used for the simulation of the $In_xGa_{1-x}N$SCs.
Band gap [10]

$$E_g(In_xGa_{1-x}N) = E_g(GaN).(1-x) + E_g(InN).x - x(1-x).b \quad (23)$$

$$E_g(In_xGa_{1-x}N) = 3.42(1-x) + 0.72x - x(1-x).b \quad , b = 1.43 \quad (24)$$

Electron affinity [11, 12]:

$$AE\ (x) = 4.1 + 0.7(3.4 - (x)) \quad (25)$$

Absorption coefficient [12] :

$$\alpha\,(x,\lambda) = 2.2.105\sqrt{(1{,}24/\lambda) - \mathrm{Eg(x)}} \quad (26)$$

Carrier mobility[13] :

$$\mu\mathrm{i}\,(N) = \mu min,+\,[(\,\mu max,i - \mu min,i)\,/1 + (\mathrm{N/Ng,i})^{\gamma \mathrm{i}}] \quad (27)$$

Effective density of states in the conduction band [11]:

$$N_{\mathrm{C}}\,(x) = 0.9x + 2.3(1-x)^{*} \quad (28)$$

Effective density of states in the valence band [11]:

$$N\mathrm{V}\,(x) = 5.3x + 1.8(1-x)^{*} \quad (29)$$

Relative permittivity [12]:

$$\varepsilon\mathrm{r}\,(x) = 14.6x + 10.4(1-x)^{*} \quad (30)$$

The above formulae with asterisk (*) are obtained from the linear fitting of the corresponding parameters of InNandGaN. The carrier mobility of InGaN is assumed to be similar to GaN, where i= n, p denotes electrons and holes,respectively, and N the doping concentration, while the model parameters $\mu max,i$, $\mu min,i$, Ng,i and γidepend on the type of semiconductor [13].

Table 1. Model parameters used in the calculations of the carrier mobility.

Type of carriers	$\mu max,i$ ($cm^2\ V^{-1}\ S^{-1}$)	$\mu min,i$ ($cm^2\ V^{-1}\ S^{-1}$)	Ng,i	γi
electrons	100	55	$2E^{17}$	1
Holes	170	3	$3E^{17}$	2

3.3. Parameters of the solar cellstudy based on $In_xGa_{1-x}N$

Surface recombination rates [14]: Spo=Sp1=Sno=Snl=1000cm/s, the reflection coefficients of the front and rear surfaces [15, 16]: RBo=RB1=0,1; both front and back contacts are assumed to be ohmic. In simulation, InGaN is treated as a perfect semiconductor. However, we have:

$$\mathrm{Egu} = \mathrm{Egop} = \mathrm{Eg} \quad (31)$$

whereEgu is the mobility gap and Egop the optical gap, usually Egu≠Egopfor non-perfect semiconductors. Assuming complete ionization of the internal doping, therefore n=ND for n-type doping and p=NA for p-type doping. Indirect recombination (SHR recombination) related to impurities are not considered in InGaN solar cell simulation. The InGaN solar cell simulation parameters are listed in Table 2.

Table 2. Simulation parameters of InGaN dual-junction solar cells at room temperature (T = 300K).

Type ofsc	layers	X	E_g(ev)	χ(ev)	N_C(10^{-19}cm^{-1})	Nv(10^{-19}cm^{-1})	εr	N_D(10^{-17}cm^{-3})	N_A(10^{-17}cm^{-3})	μn cm^{-2}V^{-1}s^{-1})	μp(cm^{-2}V^{-1}s^{-1})	D(nm)
	P1	0.52	1.64	5.33	1.57	3.62	12.58	0	1	685	153.3	30
	n1	0.52	1.64	5.33	1.57	3.62	12.58	1	0	685	153.3	100
	p2	0.84	0.94	5.82	1.12	4.74	13.93	0	1	685	153.3	30
	n2	0.84	0.94	5.82	1.12	4.74	13.93	1	0	685	153.3	100

4. Results and discussion

In this paper we study the effect of concentration ratio the output parameters of the solar cell exposed to AM 1.5. The external parameters are: the short circuit (Jsc mA/cm^2), the open circuit voltage (Voc Volt) and the efficiency (η%).

The simulation results for short circuit current, Jsc [mA/cm^2], is shown in Fig. 2. The Jsc increases linearly with number of suns as expected.

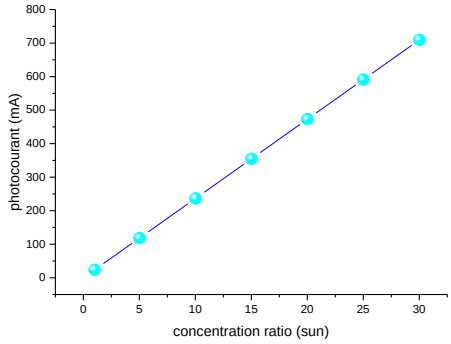

Fig. 2. Short circuit current as a function of concentration ratio.

Figs. 3 show the open circuit voltage versus the sun concentration ratio. Results show how, as we increase the solar concentration ratio, the open circuit voltage increases until reaching a value of 1.21 V for a C- ratio of 30suns.

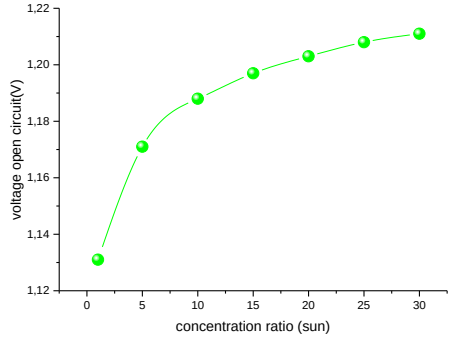

Fig. 3.Variation of open circuit voltage with concentration ratio.

The result for fill factor is shown in Fig. 4. Fill Factor decreases with number of suns but there is a nonlinear effect with finger spacing indicating possibility of optimal design.

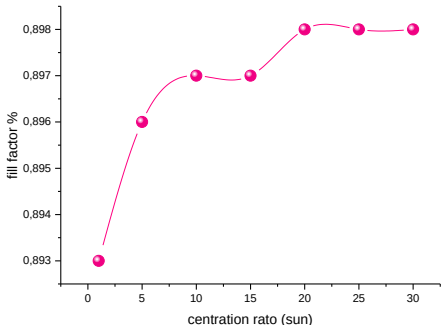

Fig. 4.Variation of Fill Factor with concentration ratio.

If we look at the Fig.5, it can be seen that as we increase the solar concentration ratio the efficiency increases until it reaches a maximum value of 25.72 % for a number of sun 30. Note that in this study the heating effect of the cell has not been considered and it might have an effect in the efficiency. This should be investigated in future work. In any case, solar cells with areas lower than1 mm side have proven to present operating temperatures below 80 ºC [14], which is the recommended maximum operating cell temperature. As a consequence, the temperature is not expecting to limit the performance of the cell with concentration if the area of the devices is kept below 1 mm x 1 mm.

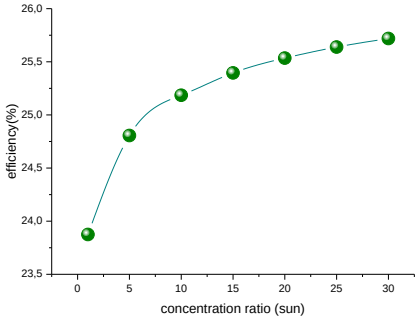

Fig. **5***Variation of efficiency with concentration ratio.*

Fig.6 illustrates the evolution of the current density depending on the voltage with different nitrogen concentrations. When the concentration in ratio increases the current density Jcc a rapid increase, on the other hand, the voltage of the open circuit a very slow increase.

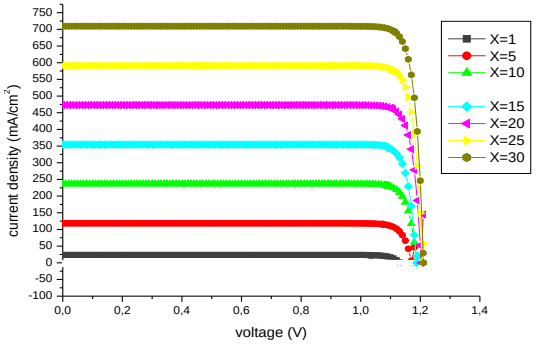

Fig. 6.Current-voltage characteristics of $In_{0.52}Ga_{0.48}N$*/* $In_{0.84}Ga_{0.16}N$ *tandem solarcell versus concentration ratio.*

5. Conclusions

A multi-junctions$In_{0.52}Ga_{0.48}N$/ $In_{0.84}Ga_{0.16}N$solar cell was calculated under low concentration (1-30suns). The conversion efficiency increases super linearly as a function of concentration. This can be explained by an increase in the minority carrier lifetime even under low concentration, since the carrier concentration in the intrinsic region is low and the high injection condition is easily achieved. High efficiency of 25.72% at 30 suns was obtained as opposed to 23.87% under lsun AM1.5 conditions.

References

[1] Mehreen Gul et al., Energy Exploration & Exploitation **34**(4), 485 (2016).
[2] I. M. Peters, S. Sofia, J. Mailoa, T. Buonassisi,RSC Adv. **6**, 66911 (2016).
[3] B. W. Liou, Solar Energy Materials & Solar Cells **114**, 141 (2013).
[4] DennaiBenmoussa, H. Benslimane, H. Khachab, Energy Procedia **139**, 731 (2017)..
[5] A. Talhi, M. Boukais, B. Dennai, A. ouldabbes, Journal of Ovonic Research **15**(3), 157 (2019).
[6]Hassane ben Slimane, Ben Moussa Dennai, HelmaouiAbderrachid,Telkomnika**12**(7), 4928 (2014)
[7] Geoffrey S. Kinsey et al., Prog. Photovolt: Res. Appl. **16**, 503 (2008).
[8] J. Nelson, The Physics of Solar Cells, Imperial College Press, London, UK 2003.
[9] A. W. Walker, Bandgap Engineering of Multijunction Solar Cells Using Nanostructures for Enhance Performance Under Concentrated Illumination, PhD Thesis, Canada 2013.
[10] Omar Souilah, A. Benzair, et al., J. Nano- Electron. Phys. **10**(4), 04013 (2018).
[11] H. Hamzaoui, A. S. Bouazzi, B. Rezig, Sol. Energy Mater. Sol. Cells **87**, 595 (2005).
[12] M. E. Levinshtein, S. L. Rumyantsev, M. S. Shur, Properties of Advanced Semiconductor Materials,Wiley, Chichester,UK, 1 (2001).
[13]T.T. Mnatsakanov, M.E. Levinshtein, L.I. Pmortseva, S.N. Yurkov, G.S. Simin, M.A. Khan, Solid-State Electron. **47**, 111 (2003).
[14] B. Hassane, D. Benmoussa, 2017 5th International Conference on Electrical Engineering – Boumerdes (ICEE-B),Boumerdes, 2017, pp. 1.
[15]A. Valera, E. F. Fernández, P. Rodrigo, F. Almonacid, IEEE 12th Spanish Conference of Electronic Devices (2018), Salamanca (Spain).